AMERICAN SOCIETY FOR MICROBIOLOGY | mBio®

RESEARCH ARTICLE
Molecular Biology and Physiology

RadD Contributes to R-Loop Avoidance in Sub-MIC Tobramycin

Veronica Negro,[a,b] Evelyne Krin,[a] Sebastian Aguilar Pierlé,[a] Thibault Chaze,[c] Quentin Giai Gianetto,[c,d] Sean P. Kennedy,[e] Mariette Matondo,[c] Didier Mazel,[a] Zeynep Baharoglu[a]

[a]Département Génomes et Génétique, Institut Pasteur, UMR3525, CNRS, Unité Plasticité du Génome Bactérien, Paris, France
[b]Sorbonne Université, Collège Doctoral, Paris, France
[c]Plateforme Protéomique, CNRS USR 2000, Institut Pasteur, Unité de Spectrométrie de Masse pour La Biologie, Paris, France
[d]Bioinformatics and Biostatistics HUB, Center of Bioinformatics, Biostatistics and Integrative Biology (C3BI), USR CNRS 3756, Institut Pasteur, Paris, France
[e]Center of Bioinformatics, Biostatistics and Integrative Biology (C3BI), Institut Pasteur, USR 3756 CNRS, Paris, France

ABSTRACT We have previously identified *Vibrio cholerae* mutants in which the stress response to subinhibitory concentrations of aminoglycoside is altered. One gene identified, VC1636, encodes a putative DNA/RNA helicase, recently named RadD in *Escherichia coli*. Here we combined extensive genetic characterization and high-throughput approaches in order to identify partners and molecular mechanisms involving RadD. We show that double-strand DNA breaks (DSBs) are formed upon subinhibitory tobramycin treatment in the absence of *radD* and *recBCD* and that formation of these DSBs can be overcome by RNase H1 overexpression. Loss of RNase H1, or of the transcription-translation coupling factor EF-P, is lethal in the *radD* deletion mutant. We propose that R-loops are formed upon sublethal aminoglycoside treatment, leading to the formation of DSBs that can be repaired by the RecBCD homologous recombination pathway, and that RadD counteracts such R-loop accumulation. We discuss how R-loops that can occur upon translation-transcription uncoupling could be the link between tobramycin treatment and DNA break formation.

IMPORTANCE Bacteria frequently encounter low concentrations of antibiotics. Active antibiotics are commonly detected in soil and water at concentrations much below lethal concentration. Although sub-MICs of antibiotics do not kill bacteria, they can have a major impact on bacterial populations by contributing to the development of antibiotic resistance through mutations in originally sensitive bacteria or acquisition of DNA from resistant bacteria. It was shown that concentrations as low as 100-fold below the MIC can actually lead to the selection of antibiotic-resistant cells. We seek to understand how bacterial cells react to such antibiotic concentrations using *E. coli*, the Gram-negative bacterial paradigm, and *V. cholerae*, the causative agent of cholera. Our findings shed light on the processes triggered at the DNA level by antibiotics targeting translation, how damage occurs, and what the bacterial strategies are to respond to such DNA damage.

KEYWORDS DNA repair, R-loop, antibiotic resistance

Bacteria frequently encounter low concentrations (sub-MICs) of antibiotics, and recent studies point to a key role of such concentrations for the genesis of resistance mutants or exogenous resistance acquisition (1). Active antibiotics are commonly detected in soil and water. Concentrations of these antibiotics are well below the MIC but nevertheless can be found at up to several hundred nanograms/liter (2). Although sub-MICs of antibiotics do not kill bacteria, they can have a major impact on bacterial populations. In particular, it was shown that concentrations as low as 100-fold below the MIC can lead to the selection of antibiotic-resistant cells (3) through the

Citation Negro V, Krin E, Aguilar Pierlé S, Chaze T, Giai Gianetto Q, Kennedy SP, Matondo M, Mazel D, Baharoglu Z. 2019. RadD contributes to R-loop avoidance in sub-MIC tobramycin. mBio 10:e01173-19. https://doi.org/10.1128/mBio.01173-19.

Editor Jeff F. Miller, UCLA School of Medicine

Address correspondence to Didier Mazel, mazel@pasteur.fr, or Zeynep Baharoglu, zeynep.baharoglu@pasteur.fr.

V.N. and E.K. contributed equally.

This article is a direct contribution from a Fellow of the American Academy of Microbiology. Solicited external reviewers: H. Seifert, Northwestern University Feinberg School of Medicine; Ivan Matic, INSERM 1001; Christophe Herman, Baylor College of Medicine.

Received 17 May 2019
Accepted 5 June 2019
Published 2 July 2019

induction of various stress responses (1, 4). SOS is one such response, triggered by a genotoxic alarm signal: single-stranded DNA, which usually results from DNA damage and/or DNA replication blockage (5). We previously found that concentrations as low as 1% of the MIC of various families of antibiotics, even those that do not cause DNA damage, such as aminoglycosides (AG), induce the SOS response in *Vibrio cholerae* and other pathogenic Gram-negative bacteria from different genera (6, 7). Notably, they also increase the mutation frequency and activate the oxidative stress and the RpoS general stress response pathways in both *V. cholerae* and *Escherichia coli*, which can lead to antibiotic resistance (6, 8). Reactive oxygen species (ROS) production was also shown to be central and ultimately to lead to replication and transcription stalling, triggering the SOS pathway (6, 9, 10). Aminoglycosides (such as tobramycin [TOB]) are bactericidal antibiotics that target the ribosome and prevent translation. Sub-MIC aminoglycosides nevertheless trigger the formation of DNA damage, evidenced by induction of SOS (6, 7). A genetic screen developed in our laboratory led to the identification of *V. cholerae* mutants in which the induction of SOS by aminoglycosides is altered (9). A number of the identified genes are involved in replication, recombination, and repair functions, suggesting that sublethal antibiotic stress is sufficient to interfere with the DNA repair and replication machineries and with RNA metabolism. Interestingly, our screen selected for mutants inactivated for the expression of proteins known to destabilize the RNA polymerase (RNAP) complex, such as Mfd. Mfd couples transcription arrests with repair by removing stalled or backtracked RNAP at bulky lesions and recruits the nucleotide excision repair (NER) machinery in a process called transcription-coupled repair (TCR) (11, 12). Stalled elongation complexes can prevent the access of DNA repair enzymes and cause replication-transcription collision. Such complexes also promote formation of structures that constitute further impediments for replication, such as R-loops. Mfd can also dislodge RNAP that pauses at abasic sites due to, for example, base excision repair of oxidative lesions (13). This is of particular interest in the case of Mfd in the response to sub-MIC tobramycin (TOB), as sub-MIC TOB treatment favors incorporation of oxidized bases into DNA (6).

In addition to Mfd, our genetic screen identified the VC1636 gene (9), which encodes a putative DNA/RNA helicase. A homolog of VC1636 was in parallel named RadD in *E. coli* and was shown to carry conserved helicase and DNA binding motifs (14). The closest RadD homolog was found to be the human XPB, a superfamily 2 helicase involved in transcription-coupled repair. *E. coli* and *V. cholerae* RadD proteins are 65% similar (58% identical), including helicase domains. RadD was identified recently by Cox and collaborators in a screen for genes involved in the response to ionizing radiation (15) and was suggested to have a role in DNA double-strand break (DSB) repair in *E. coli* (14, 16). We have identified *V. cholerae* VC1636 RadD as involved in the response to sub-MIC tobramycin stress. VC1636 RadD overexpression, from a high-copy-number plasmid, was able to restore survival of UV in an otherwise UV-sensitive *mfd* mutant (9), leading to the hypothesis that RadD could have a similar function as Mfd in removing stalled RNAP. A subsequent study from the Cox laboratory showed that RadD interacts with the *E. coli* single-stranded DNA binding protein SSB, which stimulates the ATPase activity of RadD (17), and that RadD can bind single-stranded DNA. However, the authors observed no *in vitro* helicase activity.

Here we combined high-throughput approaches and genetic characterization of multiple mutants to address the precise role of the *E. coli* and *V. cholerae* RadD proteins. For the genetic study, we focused on *E. coli*, since previous studies were conducted primarily in *E. coli* and due to the fact that *V. cholerae* mutants with impaired DNA double-strand break repair had poor viability. We show that sub-MIC tobramycin treatment leads to formation of double-strand DNA breaks (DSBs) in the absence of *radD* and that RNase H1 overexpression counteracts such DSB formation. Importantly, we find that the viability of the *radD* deletion mutant strongly relies on RNase H1 function. We further show that RadD directly interacts with the homologous recombination (HR) helicase RecQ. We propose that sublethal aminoglycoside treatment leads

to R-loop-dependent formation of DSBs, which can be repaired by the RecBCD homologous recombination pathway, and that RadD counteracts such R-loop accumulation.

RESULTS

TI-seq identifies *rnhA* inactivation as highly detrimental in *V. cholerae radD*. In order to characterize RadD, we addressed its effect in the presence of tobramycin. We adopted a high-throughput transposon insertion sequencing (TI-seq) approach to determine which genes are important in maintaining the cell integrity in the presence of antibiotics at low doses in the *radD* strain. We chose to perform the TI-seq experiments in *Vibrio cholerae*, because the changes caused by sub-MIC tobramycin are more marked in this species than in *E. coli* (6, 18), and *radD* was identified in the response to TOB in *V. cholerae* (9). Large transposon inactivation libraries in *V. cholerae* wild-type (WT) and *radD* strains were subjected to growth for 16 generations in medium without and with TOB at 50% of the MIC (0.6 μg/ml). After sequencing, insertion detection, mapping, and counts (see Text S1 in the supplemental material), we identified genes where detected insertions had at least a 4-fold increase or decrease in the *radD* strain and not in the WT after 16 generations (Table 1). We also identified genes with differential detection of insertions at T_0 in the *radD* strain (Table 2). The genes marked with an asterisk in Table 2 were subsequently deleted in our WT and (when possible) in *radD V. cholerae* strains to confirm the fitness effect revealed by TI-seq (Fig. S1).

Strikingly, the number of detected insertions in *rnhA* coding for RNase H1 at T_0 decreased 4.4-fold in the *radD* mutant compared to WT (Table 2), and *rnhA* inactivation was found to be highly detrimental in the *radD* strain after 16 generations in Mueller-Hinton (MH) (loss of 5.9-fold in *radD* mutant against 1.7-fold in WT) and even more so in TOB (loss of 13.5-fold in *radD* mutant against 1.6-fold in WT). We constructed single mutants of *rnhA* in *V. cholerae* WT; however, despite our efforts, we could not delete *rnhA* in the *V. cholerae radD* mutant (not shown). We took advantage of a thermosensitive plasmid expressing $radD_{vc}$ to construct *rnhA* deletion mutants at a permissive temperature in *V. cholerae* WT and *radD* mutant contexts, but the double mutant strains did not grow upon loss of plasmid at a nonpermissive temperature, suggesting synthetic lethality with *radD* under these conditions (Fig. S1J). In parallel, we applied a similar strategy in *E. coli* using P1 transduction of *rnhA* interrupted by a resistance cassette and found that the *E. coli radD rnhA* mutant could also not be constructed at a nonpermissive temperature (Fig. S1K). These results show the importance of processing R-loops in the absence of RadD and are consistent with a role of RadD related to R-loop formation/destabilization.

Importance of genes related to DNA metabolism in the *V. cholerae radD* mutant. At time zero and T_{16}, a large proportion of the genes that are specifically found to be important for the *radD* strain during antibiotic stress are involved in energy metabolism, general metabolism, and membrane integrity (Tables 1 and 2), among which are two operons that become essential in the *radD* strain (no insertions detected), the proton-motive-force-dependent *tol-pal* operon ensuring membrane integrity (19) and the *ngr* operon involved in oxidative stress (20), suggesting that the *radD* strain is more sensitive to oxidative and membrane stresses. Another category includes genes related to DNA metabolism (*polA, mutT, apaH*), suggesting the increased occurrence of DNA damage in the *radD* strain. PolI (*polA*) is a DNA polymerase responsible for stripping RNA primers during lagging-strand replication but is also pivotal in various DNA repair pathways in *E. coli* (21, 22). ApaH is involved in detoxification of toxic DNA bases (23) and resistance to stress (24), and MutT limits incorporation of potentially mutagenic oxidized guanine residues into DNA (25). Interestingly, *mutT* inactivation detection decreased 13.6-fold in the TI-seq experiment in *radD* TOB compared with only 2.4-fold in WT TOB. Moreover, as described above for the *rnhA radD* synthetic lethality, the *polA radD* double mutant could also not be obtained in *V. cholerae* using the same strategy (not shown). The identification of these genes points to amplified DNA damage in the absence of *radD* and suggests that the *radD* strain is somehow less tolerant to oxidative variations (even in the absence of TOB) and could have difficulties

TABLE 1 Genes where insertions are specifically lost or enriched in the *radD* strain after evolution in MH or TOB

Decrease or increase[e] and antibiotic	Gene ID		Role	Fold change for T_{16} vs T_0 (P value) for strain:			
	Locus tag	Name		MH *radD* strain[a]	MH WT[b]	TOB *radD* strain[c]	TOB WT[d]
Decrease							
No antibiotic	VC1835	*pal*	Outer membrane integrity	No reads (0)	−1.8		
	VC1837*	*tolA*	Outer membrane integrity	No reads (0)	8.3		
	VC1838	*tolR*	Outer membrane integrity	No reads (0)	5.9		
	VC1839	*tolQ*	Outer membrane integrity	No reads (0)	−1.2		
	VC2291	*ngrE*	Iron and oxidative stress	No reads (0)	6.2		
	VC2292	*ngrD*	Iron and oxidative stress	No reads (0)	1.1		
	VC2293	*ngrC*	Iron and oxidative stress	No reads (0)	1.2		
	VC2294	*nqrB*	Iron and oxidative stress	No reads (0)	5.1		
	VCA0897	*pgl*	Pentose phosphate pathway	−26.3 (0.009)	2.1		
	VCA0609		Unknown	−23.4 (1.60E−15)	2.9		
	VCA0634		Putative tRNA modification	−9.3 (0.011)	1.5		
	VC2517		Putative ABC-type transport	−6.7 (1.00E−08)	1.5		
	VC2234*	*rnhA*	RNase H1, R-loop degradation	−5.9 (0.014)	−1.7		
	VC1575		Unknown	−4.1 (4.50E−07)	−1.7		
TOB, 50% MIC	VC1948		Unknown	1.6	−1.5	−30.9 (0.001)	−1.2
	VC0678	*hlyU*	Transcriptional regulator	−2.9	−3.2	−16.8 (0.001)	1.3
	ncRNA235		Noncoding RNA	−1.3	2	−16.2 (0.006)	−1.8
	VC2392*	*mutT*	Nucleotide detoxification	1	−1.8	−13.6 (8.70E−05)	−2.4
	VC2234*	*rnhA*	R-loop degradation	−5.9	−1.7	−13.5 (0.002)	−1.6
	VCA0569	*vxrE*	Unknown	−1.8	1.8	−10.3 (1.90E−04)	1.2
	VC2718	*bioH*	Metabolism	1.9	1.2	−8.7 (1.50E−04)	−2.2
	VC1759		Prophage integrase	−1.1	1.3	−8 (0.001)	1.6
	VCA0032		Unknown	−2.8	−1.4	−5.6 (2.20E−04)	−1.5
	VCA0741		Unknown	1.8	2.2	−5 (0.008)	−1.3
	VCA0654	*scrR*	Carbohydrate metabolism	−1.6	2.1	−4.9 (5.80E−05)	−1.2
	VC0099	*glpG*	Protease	1.3	−1.6	−4.8 (3.70E−06)	−1.5
	VC1824		Carbohydrate metabolism	−1.3	−1.7	−4.5 (0.004)	−1.1
	VCA0608	*yjjG*	Nucleotide detoxification	−1.2	2.1	−4.2 (1.90E−05)	−1
	VCA0501		Unknown	1.3	1.5	−4.1 (2.60E−11)	1.9
Increase							
No antibiotic	VC0887*	*yqcC*	Pseudouridine synthase (Hyp)	8.3 (0.045)	2.9		
	VC0330	*rsd*	Putative transcription factor	6.5 (0.003)	1.1		
	VC1167	*tdk*	Pyrimidine metabolism	4.7 (7.20E−09)	2.7		
TOB, 50% MIC	VC1262		Putative methyltransferase	−1.1	1.3	6.4 (3.00E−05)	1.7
	VC1150		Unknown	2.4	1.2	4.8 (1.00E−04)	2.1

[a]Average insertions detected in MH *radD* strain at T_{16} compared to *radD* strain at T_0; all numbers express fold changes.
[b]Insertions in MH WT at T_{16} compared to WT T_0.
[c]Average insertions detected in TOB *radD* strain at T_{16} compared to *radD* strain at T_0.
[d]Average insertions detected in TOB WT at T_{16} compared to WT T_0. Genes with at least 4-fold changes are shown. Deletions for genes marked with an asterisk were constructed in *V. cholerae* WT and *radD* strains.
[e]In *radD* strain but not WT at time T_{16}.

coping with the incorporation of modified nucleotides in DNA (or RNA) compared with the WT. These results do not exclude, however, the occurrence of such stress in the WT context upon TOB treatment, consistent with our previous results showing the importance of MutT in response to sub-MIC tobramycin in *V. cholerae* (6). Subsequent growth assays indeed show that deletion of *mutT* causes a slight growth defect in both WT and *radD* strains (Fig. S1M). Several gene inactivations whose detections increase in *radD* were also identified (Tables 1 and 2). We constructed simple and *radD* double deletion mutants for several such genes, i.e., YqcC, putative tRNA pseudouridine synthase; RdgC, which inhibits RecA-mediated strand exchange *in vitro* (26); and YebG, belonging to the SOS regulon and DSB processing pathways (27), but we observed no significant effect on growth in either MH or TOB (not shown), although they appear to slightly increase the MIC of TOB (Fig. S1L). Further study needs to be carried out to elucidate the interplay between RadD and these factors. Finally, since RadD was previously suggested to be involved in DSB repair, we expected to find *recB* inactivation as detrimental in the *radD* context, but the stringency of our analysis did not show the loss of detected

TABLE 2 Genes with differential insertions at T_0 in *radD* strain

Change in no. of insertions in *radD* mutant at T_0 (compared to WT) and gene type	Gene ID			Normalized reads (no. of sequenced insertions) of strain at T_0		Fold change of no. of insertions in *radD* strain compared to WT, both at T_0[b]	*P* value
	Locus tag	Name	Role[e]	WT[a]	*radD* mutant		
Decrease							
DNA/RNA metabolism	VC0108	*polA*	DNA replication/repair	109	6	**19.5**	0.019
	VC0441[d]	*apaH*	Purine metabolism	400	90	**4.9**	0.007
	VC2392*[c]	*mutT*	Nucleotide detoxification	387	81	**4.8**	0.049
	VC2234*	*rnhA*	RNase H1, R-loop degradation	245	55	**4.4**	0.010
Translation	VC0443*[d]	*ksgA*	rRNA modification	215	13	**16.3**	0.019
	VC2679	*rpmE*	Ribosomal protein	513	39	**13.3**	0.075
	VC0582	*rsmI*	rRNA modification	387	44	**8.7**	0.019
	VC2660*	*efp*	Translation elongation factor	222	41	**5.4**	0.019
Other	VC0556*	*gshA*	Thiol redox system	134	2	**67.0**	0.040
	VC0824	*tpx*	Thiol redox system	560	85	**6.6**	0.022
	VC2381	*btuF*	Vitamin B12 ABC transporter	330	67	**4.9**	0.016
	VC2288	*nqrM*	Energy metabolism	314	69	**4.5**	0.016
	VC0240	*rfaD*	LPS	223	4	**59.4**	0.013
	VC1215	*pgsA*	Cell membrane integrity	208	7	**30.4**	0.042
	VC2156	*nlpC*	Outer membrane integrity	414	46	**9.0**	0.022
	VC1044		Unknown	622	53	**11.7**	0.038
	VC0300		Unknown	271	16	**16.9**	0.015
	VC0911	*treA*	Trehalose metabolism	331	31	**10.8**	0.032
	VC2669		Tyrosine metabolism	462	78	**5.9**	0.000
	VC0395	*gtaB*	Carbohydrate metabolism	446	53	**8.4**	0.043
	VC0964	*crr*	Carbohydrate metabolism	341	72	**4.7**	0.004
	VC0721	*pstS*	Phosphate ABC transporter	289	71	**4.1**	0.047
	VC1802		Unknown	516	19	**27.5**	0.011
	VC1810		Unknown	508	31	**16.5**	0.040
Increase	VC2326*	*yebG*	dsDNA-binding SOS protein	19	136	*7.2*	0.05
	VCA0156	*mrpC*	Electron transport	26	159	*6.2*	0.03
	VC0718*	*rdgC*	NAP	34	199	*5.9*	0.03
	VC1693	*torC*	Energy metabolism	59	255	*4.3*	0.05

[a]Normalized average reads.
[b]Values in boldface are decreases; values in italic are increases. These numbers correspond to fold changes calculated with average insertions that included decimals. Genes with at least 4-fold differences are shown.
[c]Deletions for genes marked with an asterisk were constructed (when possible) in *V. cholerae* WT and *radD* strains. *ksgA* mutants could not be obtained.
[d]*ksgA* and *apaH* are in the same operon.
[e]Abbreviations: LPS, lipopolysaccharide; dsDNA, double-stranded DNA; NAP, nucleotide-associated protein.

insertions in *recB* as statistically significant. This is due to the low number of initial insertions in the *recB* gene in both WT and *radD* contexts and further decreased detections after 16 generations in TOB. However, when we specifically look at the faith of detected insertions after 16 generations in the absence of TOB, the number of reads decreases 6-fold in the *radD* mutant but not in the WT, supporting the hypothesis that DSB repair is important in the absence of *radD*.

Coupling of transcription and translation is critical in *radD* mutant and in sub-MIC TOB. Another category of genes whose inactivation affects growth of the *radD* strain relates to translation, particularly ribosome biogenesis and stability factors (such as KsgA) and EF-P, a translation-transcription coupling factor (Table 2). Insertion counts decreased 5.4-fold for *efp* in the *radD* mutant at time zero compared to WT. We found that the deletion of *efp* affects the growth of *radD* even in the absence of antibiotics (Fig. S1A and B), suggesting that the coupling of transcription and translation is important in this mutant. Moreover, we observe that deletion of *efp* is lethal in TOB at 50% of the MIC, even in the *radD*$^+$ context, highlighting the need for translation-transcription coupling upon exposure to sub-MIC TOB (Fig. S1A to C).

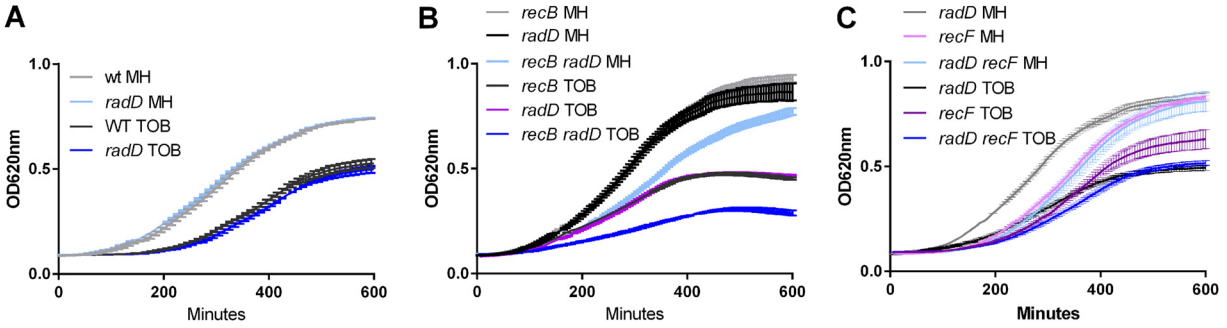

FIG 1 Growth of *E. coli* mutants in the presence of TOB at 50% of the MIC (0.25 μg/ml). Growth was measured with the Tecan Infinite plate reader. MH is rich medium without antibiotic. Each condition was tested 3 to 5 times. Standard deviations are represented. Statistical significance tests were performed on the slopes, and *P* values are represented in Table S2.

RadD directly interacts with RecQ. In parallel, in order to identify protein partners of RadD, we performed a tandem affinity purification assay (TAP-tag [Text S1] [28, 29]), under conditions with and without antibiotic stress in *V. cholerae* (data not shown). Selected proteins were then tested by yeast two-hybrid assay (30), among which was RecQ helicase. RecQ, together with SSB, has been previously identified in a TAP-tag assay with *E. coli* RadD (17), but RecQ was suggested tp be detected because of a coassociation with SSB. We observed here strong direct interaction between *V. cholerae* RadD and RecQ (Fig. S2). On the other hand, no interaction was observed between RadD and the RNA polymerase subunits RpoB/C (not shown).

The RecBCD double-strand break homologous recombination repair pathway is important in the response to tobramycin in the absence of *radD*. In parallel to the high-throughput approach, we undertook an extensive genetic study in *E. coli*, due to the fact that *V. cholerae* mutants with impaired DNA repair had poor viability. To analyze the response of different mutants to TOB, we assayed growth in TOB at 50% of the MIC (0.25 μg/ml for *E. coli*). Deletion of *radD* alone conferred no growth defect (Fig. 1A and Table S2). In order to understand which pathways could be linked with the function of RadD, we inactivated several genes related to DNA stress and repair pathways in *E. coli*: *recB* (HR, double-strand break repair), *recF* (HR, single-strand gap repair), *uvrA* (NER), *dinB* (translesion synthesis), and *rep* and *dinG,* which are accessory replicative helicases that clear DNA from roadblocks (31). We then tested growth of single and double *E. coli* mutants in MH and TOB. No negative effect was observed for deletion of *uvrA*, *dinG*, *rep,* and *dinB* in the *radD* context, in MH, or in TOB (Fig. S3), consistent with TI-seq data. This suggests that replication in the *radD* mutant is not impaired by roadblocks and bulky complexes or lesions and that NER is not needed. On the other hand, inactivation of *recB* (Fig. 1B) but not *recF* (Fig. 1C) was observed to be detrimental in the *radD* mutant. This points to DSB formation in the *radD* mutant in the presence of TOB, and even in MH without antibiotic, thus requiring RecBCD homologous recombination.

DSB formation in *E. coli recB* and *recB radD* strains was quantified using a fluorometric terminal deoxynucleotidyltransferase-mediated dUTP-biotin nick end labeling (TUNEL) assay. In this system, double-strand ends, including those generated by DSBs, are fluorescently labeled and quantified by flow cytometry. We used *recB* derivatives for this assay, so that DSBs that are formed cannot be repaired and thus can be accurately measured. Figure 2A (and Table S2 for statistical significance) shows that fluorescence is increased in the *recB radD* strain compared to the *recB* single mutant in TOB. These results are consistent with the hypothesis that DSBs are formed in the *radD* mutant in sub-MIC TOB and that these breaks are repaired by the RecBCD HR pathway.

R-loops are responsible for part of the DSBs formed in the absence of *radD* in TOB. RadD had been reported previously to be involved in DSB repair (14, 16), but no molecular mechanism was proposed. Having identified *radD* in a stalled-transcription screen (9), and based on our TI-seq data identifying *rnhA* deletion as detrimental in the

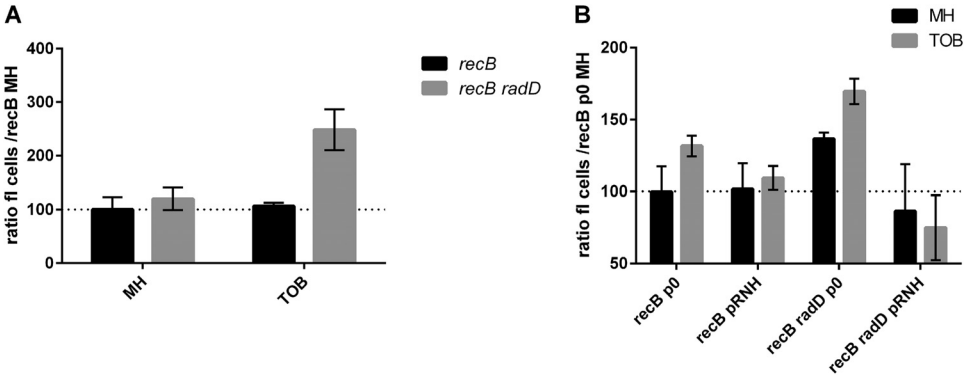

FIG 2 Quantification of DNA double-strand breaks in *E. coli*. TUNEL assays were performed (see Materials and Methods), and fluorescence was measured by flow cytometry (MACSQuant). Standard deviations are represented. Statistical significance tests (*t* tests) were performed, and *P* values are represented in Table S2. MH, no antibiotic; TOB, 0.2 μg/ml; p0, empty pTOPO vector; pRNH, pTOPO::rnhA$_{ec}$ (plasmids pB352 and pI388 are shown in Table S1).

radD mutant, we were in a position to ask the question of whether DSBs formed in the *radD* mutant could arise from R-loops. Indeed, R-loops are frequently formed under conditions where RNAP stalls (32, 33) and can be at the origin of DSB formation when they are not degraded by RNase H1 (*rnhA*) (32, 34).

In order to test this hypothesis, we first undertook the construction of various *rnhA* mutant derivatives in *E. coli*. However, as previously described (33, 35–38), all the strains carrying *rnhA* inactivation quickly accumulated suppressor mutations. A second strategy was used to look for the phenotype of RNase H1 overexpression in our different mutants: we compared growth of *E. coli recB* and *recB radD* strains transformed with a plasmid overexpressing RNase H1 or with an empty plasmid. We also tested isogenic *recB*$^+$ strains. No effect of RNase H overexpression was observed in the *recB*$^+$ context for the WT and *radD* mutant (Fig. S4). In the *recB*-deficient context, although we observed a slight improvement by RNase H1 overexpression on growth of the *recB* strain in TOB (Fig. 3A), the effect was even more marked in the *recB radD* mutant, where pRnhA$^+$ significantly improved growth (Fig. 3B).

We quantified DSB formation in the presence of the RNase H1-overexpressing plasmid in *E. coli* (Fig. 2B). Interestingly, introduction of the empty plasmid led to slightly higher DSB levels in the *recB* mutant in TOB. In the *recB radD* context with empty plasmid, DSB levels were increased compared to the *recB* strain, which was

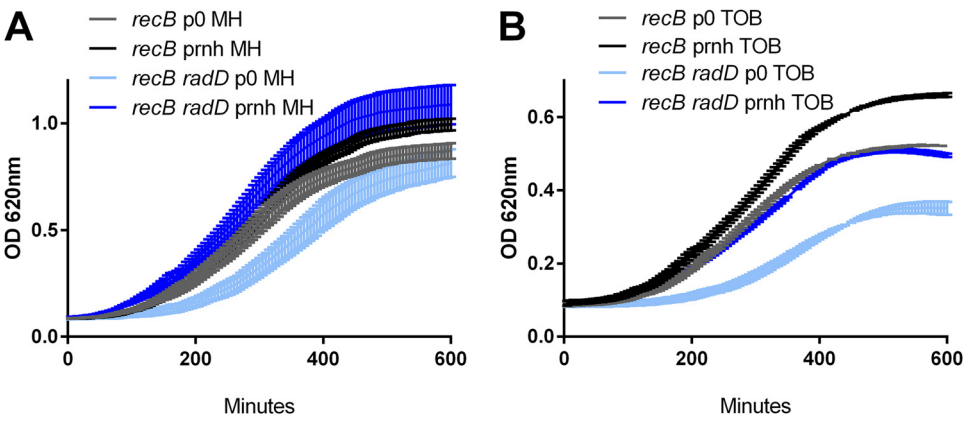

FIG 3 Effect of RNase H overexpression on growth of *E. coli* mutants in *recB*-deficient context. Growth was measured with the Tecan Infinite plate reader. MH is rich medium without antibiotic. An 0.2-μg/ml concentration of TOB was used in the *recB*-deficient context (instead of 0.25 μg/ml) because of decreased viability of *recB* mutants. Each condition was tested at least 3 times. Standard deviations are represented. Statistical significance tests were performed on the slopes, and *P* values are represented in Table S2. Plasmids are as in Fig. 2.

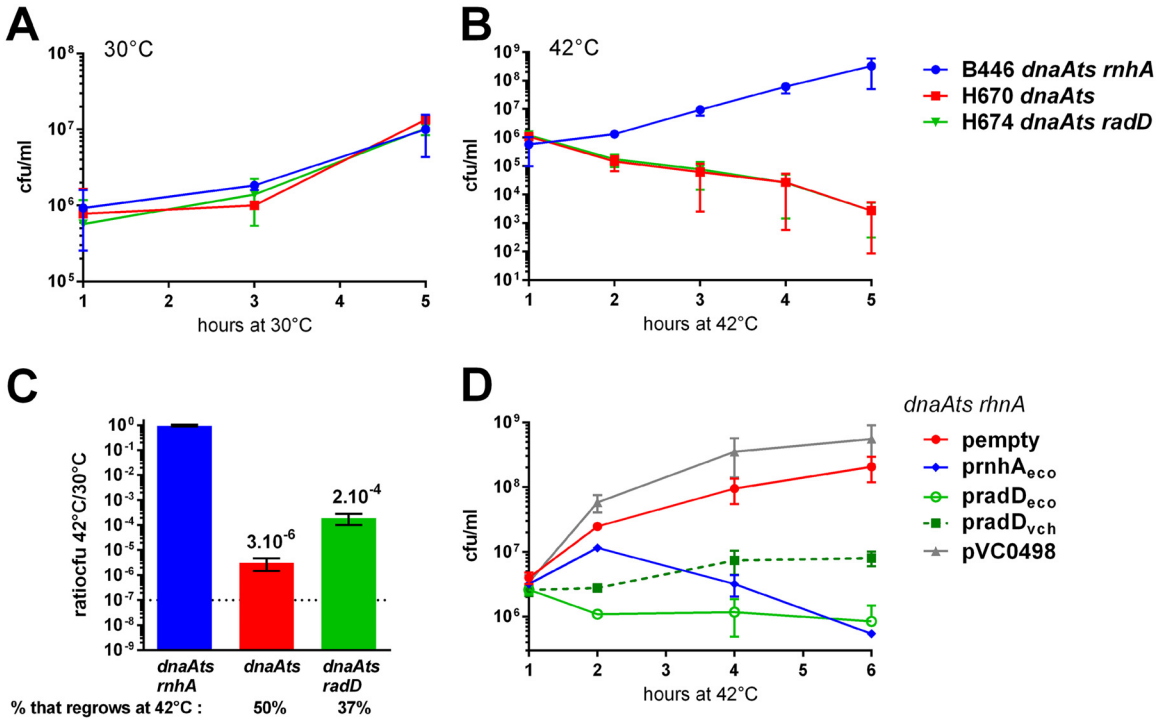

FIG 4 Effect of RadD in R-loop-dependent stable DNA replication in *E. coli dnaA*(Ts) mutant. Cultures were started at 30°C and were kept at 30°C (permissive) or shifted at 42°C (nonpermissive temperature) at time zero. (A, B, and D) Numbers of CFU are represented over time after time zero (hours). When a plasmid was present, carbenicillin (100 μg/ml) was added to the medium. (C) Overnight cultures were plated at 30°C and 42°C, and the ratios of CFU are shown. pempty, empty pTOPO vector; prnhA$_{eco}$, pradD$_{eco}$, pradD$_{vch}$, and pVC0498, plasmids expressing the corresponding genes (plasmids pB352, I388, I605, I468, and I391 are shown in Table S1).

consistent with what was observed in the plasmidless assay (Fig. 2A). When pRnhA$^+$ was introduced in the *recB radD* context, the DSB levels decreased compared to the isogenic strain with empty plasmid in TOB. These results suggest that the overexpression of RNase H1 relieves DSBs that are formed in the absence of *radD* in TOB and that R-loop formation at least partly accounts for the viability loss of the *radD* mutant, suggesting that *radD* could have a role in the avoidance/destabilization of R-loops.

RadD is involved in R-loop degradation/limitation *in vivo*. We were unable to test direct unwinding of RNA-DNA hybrids *in vitro* despite our efforts to purify an active form of *V. cholerae* RadD. In order to address whether R-loop formation is increased *in vivo* in the absence of RadD, we used the properties of the *dnaA*(Ts) *rnhA* mutant where stable DNA replication occurs at R-loops throughout the chromosome (39). As DnaA is essential for priming of chromosome replication in *E. coli*, the *dnaA*(Ts) thermosensitive mutant cannot grow at 42°C. Inactivation of RNase H1 (*rnhA*) in the *dnaA*(Ts) mutant restores viability because of increased formation of R-loops, which can prime replication initiation. We hypothesized that if R-loop formation is increased in the *radD* mutant, then the *dnaA*(Ts) *radD* strain would also grow at 42°C. Figure 4 shows that although all mutants have similar growth profiles at the permissive temperature (30°C, Fig. 4A), only the inactivation of *rnhA* restores viability at 42°C, and not *radD* (Fig. 4B). This means that the number of R-loops that are formed upon *radD* deletion is not increased to levels sufficient to promote stable replication in the *dnaA*(Ts) background. However, when these mutant strains were grown at 30°C and then restreaked at 42°C, we observed growth of several colonies in the *dnaA*(Ts) *radD* strain but not in the *dnaA*(Ts) strain. We quantified the appearance of these colonies by plating the cultures at 42°C and observed that there is an increase of CFU from 3×10^{-6} in the *dnaA*(Ts) strain to 2×10^{-4} in the *dnaA*(Ts) *radD* strain (Fig. 4C). Since spontaneous mutation frequencies were not increased in the *radD* or *radD dnaA*(Ts) strain compared to isogenic *radD*$^+$ strains (data not shown), this ~100-fold increase of spontaneously

growing colonies was unexpected. These CFU could appear due to genetic suppression mutations or to stochastic phenotypic variation. When we restreaked these CFU at 42°C, only 37% to 50% grew again, independently of the fact that the strain was deleted or not for *radD* (Fig. 4C). These results suggest that more R-loops are formed stochastically in the *radD* strain and that this phenotype cannot be inherited, meaning that at least half of the obtained CFU are not genetic suppressors. A major difference between planktonic and colony growth is oxygen availability. One possible explanation for the growth of the *radD dnaA*(Ts) strain in solid and not liquid medium could be that the strain could be particularly sensitive to oxygen and therefore will grow only in colonies that are under mostly anaerobic growth. Using a high-copy-number plasmid (~100 copies), we next addressed whether overexpression of RadD has a negative effect on R-loop formation. The *dnaA*(Ts) *rnhA* strain with empty plasmid grows at 42°C (Fig. 4D). Reintroduction of *rnhA* in *trans* prevents growth as expected, and so does overexpression of *E. coli radD* and *V. cholerae radD*. In order to ascertain that growth prevention is not due to protein overexpression, we also expressed a *V. cholerae* protein with a putative RNase function (VCA498) and found no effect on growth. Altogether, these results show that RadD overexpression has a negative effect on R-loop formation. R-loop formation is under some conditions related to DNA superhelicity levels. We tested *in vivo* whether supercoiling levels could be different in the *radD* mutant using an assay developed previously in the laboratory (40) and found that RadD has an impact on DNA topology (Fig. S5); however, chloroquine gels to test plasmid supercoiling in the presence or absence of RadD did not yield conclusive results regarding an effect of RadD on topology in this assay (not shown).

DISCUSSION

We show here that in the absence of *radD, V. cholerae* relies on various factors, such as RNase H1, for efficient response to sub-MIC TOB. The results also highlight the fact that the presence of sub-MIC TOB leads to DSBs, at least partly through R-loop formation, explaining the need for DSB repair in the absence of RadD.

In previous studies, the *E. coli radD* single mutant showed only a very small defect in survival of UV irradiation compared to the WT strain (14), unlike the UV-sensitive *mfd* mutant (41). When we further addressed the role of RadD in the response to UV damage, and a possible link with Mfd, the *radD mfd* double mutant showed higher UV sensitivity than the *mfd* single mutant, suggesting that RadD and Mfd may have overlapping functions in response to UV irradiation (not shown). The absence of these factors affects also the response to sub-MIC TOB, pointing to impaired transcription.

The link between transcription impediments, R-loop formation, and DSBs has been described in prokaryotes and eukaryotes. It is known that R-loops accumulate at stalled transcription elongation complexes (32, 33) and in the absence of effective transcription termination (42). In human cells, it was shown that R-loops provoke DSB formation by interfering with replication (43–45). In bacteria, replication-transcription collisions are known to lead to genomic instability and breaks (32, 46). Previous work has established that R-loops generate DSBs because they constitute replication blocks and that RNAP backtracking is an important factor potentiating the formation of such R-loop extensions and DSBs (32). The fact that we did not see any effect of the inactivation of replicative helicases such as Rep or DinG in the *radD* strain suggests that the absence of *radD* does not cause replication blocks. However, R-loop-dependent genome instability is not necessarily due to replication blocks. In a recent study, it was shown that R-loop-dependent DSB formation in *E. coli* was due not to replication impairment but to formation of RNA gaps at R-loops (RNA-DNA junctions at arrays of R-loops), which lead to chromosomal DSBs (34). Importantly, overexpression of RNase H1 and active antibacktracking mechanisms suppress such DSB accumulation in *E. coli* (32). Another HR helicase proposed to prevent R-loop formation is RecG (47). Deletion of *recG* is colethal with *rnhA* and promotes stable DNA replication. However, our TI-seq data predict no colethality of *recG* and *radD*, as insertions in *recG* are detected at equivalent levels in WT and *radD* strains in the presence or absence of TOB. On the

other hand, the *E. coli radD recG* mutant was previously studied (14) and the authors found that the strain rapidly accumulates suppressors and proposed that this could be due to a DSB repair defect. Here, RecG does not appear to be important in the absence of RadD, but one cannot rule out the possibility that RecG and RadD may have overlapping functions against R-loops. DSB formation could also be linked to DNA structures formed upon inappropriate R-loop processing in a *radD* mutant. R-loops can also interfere with DNA damage repair. It was shown in yeast that RNase H1 is important at DSBs against R-loops which otherwise impair recruitment of RPA (replication protein A, the SSB orthologue; SSB) and subsequent access of HR proteins to DSBs (48). Along the same line, a recent study showed that the human transcription-coupled repair protein CSB is recruited to R-loops induced by reactive oxygen species (ROS) at transcribed sites to initiate repair by HR (49).

How RadD counteracts/reduces R-loop formation is unclear. One possibility is through an effect on DNA supercoiling, which is linked to R-loop formation. In *E. coli*, TopoI is known to interact with RNAP and reduce R-loops (50) and its depletion leads to negative supercoiling behind the transcribing RNAP, enhancing R-loop formation (36). We observed that RadD has an impact on DNA topology, but this effect can also be indirect.

On the other hand, we know that RadD interacts with SSB (17) and with RecQ (this study). One possible hypothesis for RadD action would thus be that RadD together with RecQ could directly destabilize/unwind R-loops and recruit SSB at DSBs. SSB stimulates the activity of RNase H1 (51) and enhances the DNA helicase activity of RecQ in *E. coli* (52) and human cells (53, 54). RecQ can impact R-loop formation (55, 56) through effects on replisome stability at transcription-replication conflicts or direct unwinding of R-loops (57) or through changes in superhelicity (57–59). *topA* and *recQ* mutant backgrounds could be used in future work to more clearly define the role of RadD.

Interestingly, it was shown that the eukaryotic RecQ5 associates with RNAP and enforces the stability of ribosomal DNA arrays (60). Translating ribosomes also inhibit DSB formation at transcription sites (33). Indeed, slowing or blocking translation leads to DSB formation in the absence of R-loop repair (34). Thus, a role for RadD-RecQ can also be envisaged at the translation-transcription level. We can speculate that RadD could be important under conditions where translation is slow/impaired for the following reasons: (i) RadD is involved in the response to TOB, which interferes with translation; (ii) slow translation can promote R-loop formation; and (iii) our TI-seq experiment identified several translation-related factors that are important for the fitness of the *radD* mutant (Tables 1 and 2), namely, EF-P and KsgA. KsgA is a ribosome biogenesis and stability factor. EF-P counteracts ribosome pausing and maintains transcription-translation coupling (61).

Coupling of transcription and translation reduces R-loop formation in bacteria and subsequent DSB formation, as a newly transcribed RNA can be bound immediately by ribosomes (62). In *E. coli*, RNA polymerase also directly binds to ribosomal subunits *in vivo*, which could facilitate coordination of transcription and translation (63). In fact, the rate of transcription was shown to be controlled by the rate of translation (64). Slow translation leads to RNAP backtracking (65, 66). Accordingly, translation prevents transcription-related formation of DSBs (32). Transcription-translation coupling can be disrupted upon ribosome stalling (in the *efp* mutant or when aminoacyl-tRNAs are limiting [67, 68]). Notably, the EF-P transcription-translation coupling factor was identified as a suppressor of the growth defect in the *rnhA topA* mutant (69), suggesting that translation can also counteract R-loops that are formed due to accumulated negative supercoiling. Another example is the *rep uvrD* mutant, which is lethal due to conflicts between replication and transcription elongation complexes. This lethality can be suppressed by *rpo** alleles destabilizing RNAP (31) but also by mutations in EF-P (70). One hypothesis regarding the anti-R-loop action of RadD could therefore be at the level of translation-transcription coupling. Under this model, the involvement of RadD in the response to TOB effects of ribosome progression is coherent.

Here, we have initially addressed the function of RadD in response to sub-MIC

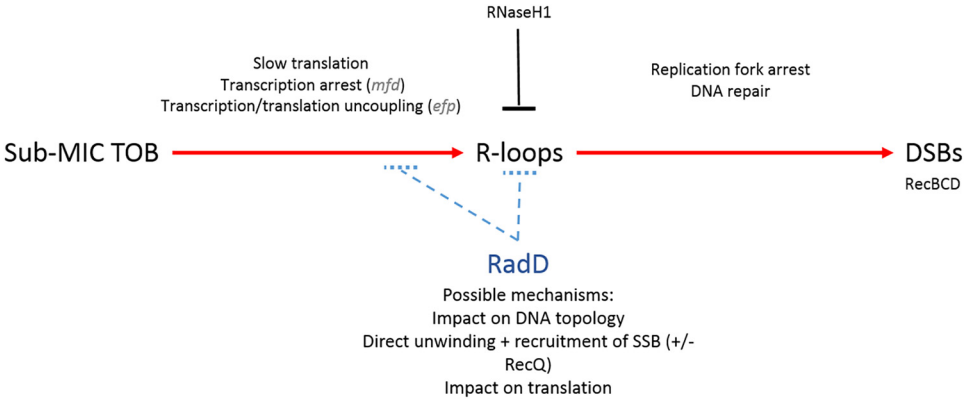

FIG 5 RadD counteracts formation of DSBs arising from R-loops. We propose that sub-MIC TOB impedes translation, leading to transcription defects, thus enhancing R-loops/R-lesions at transcription sites, causing DSBs that are repaired by the RecBCD pathway. We hypothesize that RadD (possibly with RecQ) acts either at the level of translation-transcription coupling for the avoidance of R-loop formation or directly at the R-loop before DSBs arise. Shown in parentheses are genes that are mentioned in the text and steps where they could be involved.

tobramycin. In the light of our results and the discussion above, we propose that TOB, even at sub-MIC levels, impedes translation, which primes defects in transcription, thus enhancing R-loops/R-lesions at transcription sites, causing DSBs that are repaired by the RecBCD HR pathway. SOS is indeed triggered here by DSB repair as observed previously (7, 9). We hypothesize that RadD, together with RecQ, acts either at the level of translation-transcription coupling for the avoidance of R-loop formation or directly at the R-loop before DSBs arise (Fig. 5). Further study is needed to unravel the exact mechanism of action of RadD on R-loops. Interestingly, the *radD* gene is located next to the *rsuA* gene putatively involved in ribosome assembly. Although we found no direct interaction between the RadD and RsuA proteins (two-hybrid data, not shown), we observe that the synteny is conserved among many gammaproteobacterial genera, such as *Escherichia*, *Klebsiella*, *Salmonella*, *Serratia*, and *Shewanella*. Finally, sub-MIC TOB may not affect all ribosomes equally, leading to heterogeneity of responses within a clonal population. Single-cell approaches (such as microfluidics) would be complementary and suitable in future research to compare behaviors and responses at both subpopulation and whole-population levels.

MATERIALS AND METHODS

MH medium was used for the study of the effect of sub-MIC tobramycin. TOB was aliquoted and stored at a 10-mg/ml concentration at −20°C. A fresh aliquot was used for each experiment.

Plasmids, strains, and oligonucleotides used in this study and their constructions are listed in Table S1 in the supplemental material. *E. coli* mutants were constructed by P1 transduction, and *V. cholerae* mutants were constructed by homologous recombination after natural transformation or with a conjugative suicide plasmid (pMP7 = pWS7848) as described previously (6, 71, 72).

Growth kinetics were performed from overnight cultures from single colonies, using the Tecan Infinite plate reader on 96-well plates for 10 h at 37°C with shaking. OD_{620} was measured every 5 min.

Growth curves (CFU counts) of the *dnaA*(Ts) derivatives were performed as previously described (9).

Double-strand break quantification was performed using the Promega fluorometric TUNEL system. An overnight culture was diluted 100× in MH with or without 0.2 μg/ml TOB and grown to an OD_{620} of 1. Carbenicillin (100 μg/ml) was added to the growth medium for plasmid-carrying strains. One milliliter (3×10^6 to 5×10^6 cells) was centrifuged at 2,000 rpm for 15 min at 4°C, washed twice with cold PBS, and resuspended in 500 μl PBS. Cells were fixed with 5 ml 1% methanol-free formaldehyde on ice for 20 min, washed twice with cold PBS, and permeabilized overnight with 5 ml ice-cold 70% ethanol. Cells were then washed twice with PBS and stained according to the manufacturer's recommendations. Green fluorescence was measured on a Miltenyi MACSQuant flow cytometer.

Transposon insertion sequencing libraries were prepared as previously described (9, 73) to achieve a library size of 600,000 clones and subjected to passaging in MH and MH with TOB at 0.5 μg/ml for 16 generations. Sequencing and analysis are described in detail in the supplemental material (see Text S1). Briefly, sequencing libraries were prepared using Agilent's Sureselect XT2 kit with custom RNA baits designed to hybridize the extremities of the Mariner transposon. Illumina paired-end sequencing technology was used, producing 2- by 125-bp-long reads. Reads were filtered through transposon mapping to ensure the presence of an informative transposon/genome junction as described previously

(74). Expansion or decrease of fitness of mutants was calculated in fold change with normalized insertion numbers (75). Baggerly's test on proportions (76) was used to determine statistical significance, and Bonferroni correction was applied for multiple testing.

Accession number(s). Accession numbers for the TI-seq reads are SRR8361877, SRR8361874, SRR8361875, SRR8361872, SRR8361873, SRR8361870, SRR8361871, SRR8361878, and SRR8361876 for the *radD* strain and SRR8351961, SRR8351962, SRR8351957, SRR8351958, SRR8351959, SRR8351960, SRR8351965, SRR8351966, SRR8351963, SRR8351964, SRR8351967, and SRR8351968 for the WT strain.

SUPPLEMENTAL MATERIAL

Supplemental material for this article may be found at https://doi.org/10.1128/mBio.01173-19.

TEXT S1, DOCX file, 0.02 MB.
FIG S1, TIF file, 0.8 MB.
FIG S2, TIF file, 0.2 MB.
FIG S3, TIF file, 0.3 MB.
FIG S4, TIF file, 0.1 MB.
FIG S5, TIF file, 0.1 MB.
TABLE S1, XLSX file, 0.03 MB.
TABLE S2, XLSX file, 0.02 MB.

ACKNOWLEDGMENTS

We thank Christophe Thomas for his help with protein purification, Melis Asal and Ricardo Albino Camacho for their participation in strain constructions, and Julie Lambert for UV tests. We thank Micheline Fromont for the yeast strains and plasmids and for her help with the two-hybrid experiment. We are grateful to Bénédicte Michel for the gift of several *E. coli* strains. We thank Melanie Blokesch for the *Vibrio cholerae* WT strain used in this study. We thank Sébastien Fleurier for advice for TUNEL experiments.

Work in the Mazel lab is funded by the Institut Pasteur, the Centre National de la Recherche Scientifique (CNRS-UMR3525), the French National Research Agency (ANR Unibac ANR-17-CE13-0010-01), and the French Government's Investissement d'Avenir program, Laboratoire d'Excellence "Integrative Biology of Emerging Infectious Diseases" (grant no. ANR-10-LABX-62-IBEID). V.N. was funded by fellowships from DIM Malinf 140051 (Conseil régional d'Île-de-France) and FRM grant DBF20160635736. S.A.P. was supported by a postdoctoral fellowship from the Roux Foundation (Institut Pasteur), the FRM grant DBF20160635736, and the ANR Unibac ANR-17-CE13-0010-01.

REFERENCES

1. Andersson DI, Hughes D. 2014. Microbiological effects of sublethal levels of antibiotics. Nat Rev Microbiol 12:465–478. https://doi.org/10.1038/nrmicro3270.
2. Jones-Lepp TL. 2006. Chemical markers of human waste contamination: analysis of urobilin and pharmaceuticals in source waters. J Environ Monit 8:472–478. https://doi.org/10.1039/b512858g.
3. Gullberg E, Cao S, Berg OG, Ilbäck C, Sandegren L, Hughes D, Andersson DI. 2011. Selection of resistant bacteria at very low antibiotic concentrations. PLoS Pathog 7:e1002158. https://doi.org/10.1371/journal.ppat.1002158.
4. Blazquez J, Rodriguez-Beltran J, Matic I. 2018. Antibiotic-induced genetic variation: how it arises and how it can be prevented. Annu Rev Microbiol 72:209–230. https://doi.org/10.1146/annurev-micro-090817-062139.
5. Baharoglu Z, Mazel D. 2014. SOS, the formidable strategy of bacteria against aggressions. FEMS Microbiol Rev 38:1126–1145. https://doi.org/10.1111/1574-6976.12077.
6. Baharoglu Z, Krin E, Mazel D. 2013. RpoS plays a central role in the SOS induction by sub-lethal aminoglycoside concentrations in *Vibrio cholerae*. PLoS Genet 9:e1003421. https://doi.org/10.1371/journal.pgen.1003421.
7. Baharoglu Z, Mazel D. 2011. *Vibrio cholerae* triggers SOS and mutagenesis in response to a wide range of antibiotics: a route towards multiresistance. Antimicrob Agents Chemother 55:2438–2441. https://doi.org/10.1128/AAC.01549-10.
8. Gutierrez A, Laureti L, Crussard S, Abida H, Rodríguez-Rojas A, Blázquez J, Baharoglu Z, Mazel D, Darfeuille F, Vogel J, Matic I. 2013. Beta-lactam antibiotics promote bacterial mutagenesis via an RpoS-mediated reduction in replication fidelity. Nat Commun 4:1610. https://doi.org/10.1038/ncomms2607.
9. Baharoglu Z, Babosan A, Mazel D. 2014. Identification of genes involved in low aminoglycoside-induced SOS response in *Vibrio cholerae*: a role for transcription stalling and Mfd helicase. Nucleic Acids Res 42:2366–2379. https://doi.org/10.1093/nar/gkt1259.
10. Baharoglu Z, Mazel D. 2014. Influence of very short patch mismatch repair on SOS inducing lesions after aminoglycoside treatment in *Escherichia coli*. Res Microbiol 165:476–480. https://doi.org/10.1016/j.resmic.2014.05.039.
11. Selby CP, Sancar A. 1993. Molecular mechanism of transcription-repair coupling. Science 260:53–58. https://doi.org/10.1126/science.8465200.
12. Selby CP. 2017. Mfd protein and transcription-repair coupling in *Escherichia coli*. Photochem Photobiol 93:280–295. https://doi.org/10.1111/php.12675.
13. Smith AJ, Savery NJ. 2008. Effects of the bacterial transcription-repair coupling factor during transcription of DNA containing non-bulky lesions. DNA Repair (Amst) 7:1670–1679. https://doi.org/10.1016/j.dnarep.2008.06.020.
14. Chen SH, Byrne RT, Wood EA, Cox MM. 2015. *Escherichia coli radD (yejH)* gene: a novel function involved in radiation resistance and double-strand break repair. Mol Microbiol 95:754–768. https://doi.org/10.1111/mmi.12885.
15. Byrne RT, Chen SH, Wood EA, Cabot EL, Cox MM. 2014. *Escherichia coli* genes and pathways involved in surviving extreme exposure to

ionizing radiation. J Bacteriol 196:3534–3545. https://doi.org/10.1128/JB.01589-14.
16. Cooper DL, Boyle DC, Lovett ST. 2015. Genetic analysis of *Escherichia coli* RadA: functional motifs and genetic interactions. Mol Microbiol 95:769–779. https://doi.org/10.1111/mmi.12899.
17. Chen SH, Byrne-Nash RT, Cox MM. 2016. *Escherichia coli* RadD protein functionally interacts with the single-stranded DNA-binding protein. J Biol Chem 291:20779–20786. https://doi.org/10.1074/jbc.M116.736223.
18. Baharoglu Z, Garriss G, Mazel D. 2013. Multiple pathways of genome plasticity leading to development of antibiotic resistance. Antibiotics (Basel) 2:288–315. https://doi.org/10.3390/antibiotics2020288.
19. Rassam P, Long KR, Kaminska R, Williams DJ, Papadakos G, Baumann CG, Kleanthous C. 2018. Intermembrane crosstalk drives inner-membrane protein organization in *Escherichia coli*. Nat Commun 9:1082. https://doi.org/10.1038/s41467-018-03521-4.
20. Koo M-S, Lee J-H, Rah S-Y, Yeo W-S, Lee J-W, Lee K-L, Koh Y-S, Kang S-O, Roe J-H. 2003. A reducing system of the superoxide sensor SoxR in *Escherichia coli*. EMBO J 22:2614–2622. https://doi.org/10.1093/emboj/cdg252.
21. Su K-Y, Lin L-I, Goodman SD, Yen R-S, Wu C-Y, Chang W-C, Yang Y-C, Cheng W-C, Fang W-H. 2018. DNA polymerase I proofreading exonuclease activity is required for endonuclease V repair pathway both in vitro and in vivo. DNA Repair (Amst) 64:59–67. https://doi.org/10.1016/j.dnarep.2018.02.005.
22. Lovett ST. 2011. The DNA exonucleases of *Escherichia coli*. EcoSal Plus 4. https://doi.org/10.1128/ecosalplus.4.4.7.
23. Farr SB, Arnosti DN, Chamberlin MJ, Ames BN. 1989. An *apaH* mutation causes AppppA to accumulate and affects motility and catabolite repression in *Escherichia coli*. Proc Natl Acad Sci U S A 86:5010–5014. https://doi.org/10.1073/pnas.86.13.5010.
24. Leveque F, Blanchin-Roland S, Fayat G, Plateau P, Blanquet S. 1990. Design and characterization of *Escherichia coli* mutants devoid of Ap4N-hydrolase activity. J Mol Biol 212:319–329. https://doi.org/10.1016/0022-2836(90)90127-8.
25. Maki H, Sekiguchi M. 1992. MutT protein specifically hydrolyses a potent mutagenic substrate for DNA synthesis. Nature 355:273–275. https://doi.org/10.1038/355273a0.
26. Drees JC, Chitteni-Pattu S, McCaslin DR, Inman RB, Cox MM. 2006. Inhibition of RecA protein function by the RdgC protein from *Escherichia coli*. J Biol Chem 281:4708–4717. https://doi.org/10.1074/jbc.M513592200.
27. Robbins-Manke JL, Zdraveski ZZ, Marinus M, Essigmann JM. 2005. Analysis of global gene expression and double-strand-break formation in DNA adenine methyltransferase- and mismatch repair-deficient *Escherichia coli*. J Bacteriol 187:7027–7037. https://doi.org/10.1128/JB.187.20.7027-7037.2005.
28. Puig O, Caspary F, Rigaut G, Rutz B, Bouveret E, Bragado-Nilsson E, Wilm M, Séraphin B. 2001. The tandem affinity purification (TAP) method: a general procedure of protein complex purification. Methods 24:218–229. https://doi.org/10.1006/meth.2001.1183.
29. Gully D, Moinier D, Loiseau L, Bouveret E. 2003. New partners of acyl carrier protein detected in *Escherichia coli* by tandem affinity purification. FEBS Lett 548:90–96. https://doi.org/10.1016/S0014-5793(03)00746-4.
30. Fromont-Racine M, Rain JC, Legrain P. 1997. Toward a functional analysis of the yeast genome through exhaustive two-hybrid screens. Nat Genet 16:277–282. https://doi.org/10.1038/ng0797-277.
31. Baharoglu Z, Lestini R, Duigou S, Michel B. 2010. RNA polymerase mutations that facilitate replication progression in the *rep uvrD recF* mutant lacking two accessory replicative helicases. Mol Microbiol 77:324–336. https://doi.org/10.1111/j.1365-2958.2010.07208.x.
32. Dutta D, Shatalin K, Epshtein V, Gottesman ME, Nudler E. 2011. Linking RNA polymerase backtracking to genome instability in *E. coli*. Cell 146:533–543. https://doi.org/10.1016/j.cell.2011.07.034.
33. Wimberly H, Shee C, Thornton PC, Sivaramakrishnan P, Rosenberg SM, Hastings PJ. 2013. R-loops and nicks initiate DNA breakage and genome instability in non-growing *Escherichia coli*. Nat Commun 4:2115. https://doi.org/10.1038/ncomms3115.
34. Kouzminova EA, Kadyrov FF, Kuzminov A. 2017. RNase HII saves *rnhA* mutant *Escherichia coli* from R-loop-associated chromosomal fragmentation. J Mol Biol 429:2873–2894. https://doi.org/10.1016/j.jmb.2017.08.004.
35. Lin Y, Dent SYR, Wilson JH, Wells RD, Napierala M. 2010. R loops stimulate genetic instability of CTG.CAG repeats. Proc Natl Acad Sci U S A 107:692–697. https://doi.org/10.1073/pnas.0909740107.
36. Drolet M, Phoenix P, Menzel R, Masse E, Liu LF, Crouch RJ. 1995. Overexpression of RNase H partially complements the growth defect of an *Escherichia coli* delta *topA* mutant: R-loop formation is a major problem in the absence of DNA topoisomerase I. Proc Natl Acad Sci U S A 92:3526–3530. https://doi.org/10.1073/pnas.92.8.3526.
37. Itaya M, Crouch RJ. 1991. A combination of RNase H (*rnh*) and *recBCD* or *sbcB* mutations in *Escherichia coli* K12 adversely affects growth. Mol Gen Genet 227:424–432. https://doi.org/10.1007/BF00273933.
38. Kogoma T, Hong X, Cadwell G, Barnard K, Asai T. 1993. Requirement of homologous recombination functions for viability of the *Escherichia coli* cell that lacks RNase HI and exonuclease V activities. Biochimie 75:89–99. https://doi.org/10.1016/0300-9084(93)90029-R.
39. Kogoma T. 1997. Stable DNA replication: interplay between DNA replication, homologous recombination, and transcription. Microbiol Mol Biol Rev 61:212–238.
40. Loot C, Bikard D, Rachlin A, Mazel D. 2010. Cellular pathways controlling integron cassette site folding. EMBO J 29:2623–2634. https://doi.org/10.1038/emboj.2010.151.
41. Schalow BJ, Courcelle CT, Courcelle J. 2012. Mfd is required for rapid recovery of transcription following UV-induced DNA damage but not oxidative DNA damage in *Escherichia coli*. J Bacteriol 194:2637–2645. https://doi.org/10.1128/JB.06725-11.
42. Leela JK, Syeda AH, Anupama K, Gowrishankar J. 2013. Rho-dependent transcription termination is essential to prevent excessive genome-wide R-loops in *Escherichia coli*. Proc Natl Acad Sci U S A 110:258–263. https://doi.org/10.1073/pnas.1213123110.
43. Britton S, Dernoncourt E, Delteil C, Froment C, Schiltz O, Salles B, Frit P, Calsou P. 2014. DNA damage triggers SAF-A and RNA biogenesis factors exclusion from chromatin coupled to R-loops removal. Nucleic Acids Res 42:9047–9062. https://doi.org/10.1093/nar/gku601.
44. Aguilera A, Garcia-Muse T. 2012. R loops: from transcription byproducts to threats to genome stability. Mol Cell 46:115–124. https://doi.org/10.1016/j.molcel.2012.04.009.
45. Sollier J, Stork CT, García-Rubio ML, Paulsen RD, Aguilera A, Cimprich KA. 2014. Transcription-coupled nucleotide excision repair factors promote R-loop-induced genome instability. Mol Cell 56:777–785. https://doi.org/10.1016/j.molcel.2014.10.020.
46. Boubakri H, de Septenville AL, Viguera E, Michel B. 2010. The helicases DinG, Rep and UvrD cooperate to promote replication across transcription units in vivo. EMBO J 29:145–157. https://doi.org/10.1038/emboj.2009.308.
47. Hong X, Cadwell GW, Kogoma T. 1995. *Escherichia coli* RecG and RecA proteins in R-loop formation. EMBO J 14:2385–2392. https://doi.org/10.1002/j.1460-2075.1995.tb07233.x.
48. Ohle C, Tesorero R, Schermann G, Dobrev N, Sinning I, Fischer T. 2016. Transient RNA-DNA hybrids are required for efficient double-strand break repair. Cell 167:1001–1013.e7. https://doi.org/10.1016/j.cell.2016.10.001.
49. Teng Y, Yadav T, Duan M, Tan J, Xiang Y, Gao B, Xu J, Liang Z, Liu Y, Nakajima S, Shi Y, Levine AS, Zou L, Lan L. 2018. ROS-induced R loops trigger a transcription-coupled but BRCA1/2-independent homologous recombination pathway through CSB. Nat Commun 9:4115. https://doi.org/10.1038/s41467-018-06586-3.
50. Drolet M. 2006. Growth inhibition mediated by excess negative supercoiling: the interplay between transcription elongation, R-loop formation and DNA topology. Mol Microbiol 59:723–730. https://doi.org/10.1111/j.1365-2958.2005.05006.x.
51. Petzold C, Marceau AH, Miller KH, Marqusee S, Keck JL. 2015. Interaction with single-stranded DNA-binding protein stimulates *Escherichia coli* ribonuclease HI enzymatic activity. J Biol Chem 290:14626–14636. https://doi.org/10.1074/jbc.M115.655134.
52. Shereda RD, Bernstein DA, Keck JL. 2007. A central role for SSB in *Escherichia coli* RecQ DNA helicase function. J Biol Chem 282:19247–19258. https://doi.org/10.1074/jbc.M608011200.
53. Cui S, Arosio D, Doherty KM, Brosh RM, Jr, Falaschi A, Vindigni A. 2004. Analysis of the unwinding activity of the dimeric RECQ1 helicase in the presence of human replication protein A. Nucleic Acids Res 32:2158–2170. https://doi.org/10.1093/nar/gkh540.
54. Sommers JA, Banerjee T, Hinds T, Wan B, Wold MS, Lei M, Brosh RM. 2014. Novel function of the Fanconi anemia group J or RECQ1 helicase to disrupt protein-DNA complexes in a replication protein

A-stimulated manner. J Biol Chem 289:19928–19941. https://doi.org/10.1074/jbc.M113.542456.
55. Saponaro M, Kantidakis T, Mitter R, Kelly GP, Heron M, Williams H, Söding J, Stewart A, Svejstrup JQ. 2014. RECQL5 controls transcript elongation and suppresses genome instability associated with transcription stress. Cell 157:1037–1049. https://doi.org/10.1016/j.cell.2014.03.048.
56. Kanagaraj R, Huehn D, MacKellar A, Menigatti M, Zheng L, Urban V, Shevelev I, Greenleaf AL, Janscak P. 2010. RECQ5 helicase associates with the C-terminal repeat domain of RNA polymerase II during productive elongation phase of transcription. Nucleic Acids Res 38:8131–8140. https://doi.org/10.1093/nar/gkq697.
57. Chang EY-C, Novoa CA, Aristizabal MJ, Coulombe Y, Segovia R, Chaturvedi R, Shen Y, Keong C, Tam AS, Jones SJM, Masson J-Y, Kobor MS, Stirling PC. 2017. RECQ-like helicases Sgs1 and BLM regulate R-loop-associated genome instability. J Cell Biol 216:3991–4005. https://doi.org/10.1083/jcb.201703168.
58. Harmon FG, Brockman JP, Kowalczykowski SC. 2003. RecQ helicase stimulates both DNA catenation and changes in DNA topology by topoisomerase III. J Biol Chem 278:42668–42678. https://doi.org/10.1074/jbc.M302994200.
59. Usongo V, Drolet M. 2014. Roles of type 1A topoisomerases in genome maintenance in *Escherichia coli*. PLoS Genet 10:e1004543. https://doi.org/10.1371/journal.pgen.1004543.
60. Urban V, Dobrovolna J, Hühn D, Fryzelkova J, Bartek J, Janscak P. 2016. RECQ5 helicase promotes resolution of conflicts between replication and transcription in human cells. J Cell Biol 214:401–415. https://doi.org/10.1083/jcb.201507099.
61. Elgamal S, Artsimovitch I, Ibba M. 2016. Maintenance of transcription-translation coupling by elongation factor P. mBio 7:e01373-16. https://doi.org/10.1128/mBio.01373-16.
62. McGary K, Nudler E. 2013. RNA polymerase and the ribosome: the close relationship. Curr Opin Microbiol 16:112–117. https://doi.org/10.1016/j.mib.2013.01.010.
63. Fan H, Conn AB, Williams PB, Diggs S, Hahm J, Gamper HB, Jr, Hou YM, O'Leary SE, Wang Y, Blaha GM. 2017. Transcription-translation coupling: direct interactions of RNA polymerase with ribosomes and ribosomal subunits. Nucleic Acids Res 45:11043–11055. https://doi.org/10.1093/nar/gkx719.
64. Proshkin S, Rahmouni AR, Mironov A, Nudler E. 2010. Cooperation between translating ribosomes and RNA polymerase in transcription elongation. Science 328:504–508. https://doi.org/10.1126/science.1184939.
65. Zhang Y, Mooney RA, Grass JA, Sivaramakrishnan P, Herman C, Landick R, Wang JD. 2014. DksA guards elongating RNA polymerase against ribosome-stalling-induced arrest. Mol Cell 53:766–778. https://doi.org/10.1016/j.molcel.2014.02.005.
66. Artsimovitch I. 2018. Rebuilding the bridge between transcription and translation. Mol Microbiol 108:467–472. https://doi.org/10.1111/mmi.13964.
67. Roche ED, Sauer RT. 1999. SsrA-mediated peptide tagging caused by rare codons and tRNA scarcity. EMBO J 18:4579–4589. https://doi.org/10.1093/emboj/18.16.4579.
68. Subramaniam AR, Zid BM, O'Shea EK. 2014. An integrated approach reveals regulatory controls on bacterial translation elongation. Cell 159:1200–1211. https://doi.org/10.1016/j.cell.2014.10.043.
69. Usongo V, Martel M, Balleydier A, Drolet M. 2016. Mutations reducing replication from R-loops suppress the defects of growth, chromosome segregation and DNA supercoiling in cells lacking topoisomerase I and RNase HI activity. DNA Repair (Amst) 40:1–17. https://doi.org/10.1016/j.dnarep.2016.02.001.
70. Myka KK, Hawkins M, Syeda AH, Gupta MK, Meharg C, Dillingham MS, Savery NJ, Lloyd RG, McGlynn P. 2017. Inhibiting translation elongation can aid genome duplication in *Escherichia coli*. Nucleic Acids Res 45:2571–2584. https://doi.org/10.1093/nar/gkw1254.
71. Baharoglu Z, Krin E, Mazel D. 2012. Connecting environment and genome plasticity in the characterization of transformation-induced SOS regulation and carbon catabolite control of the *Vibrio cholerae* integron integrase. J Bacteriology 194:1659–1667. https://doi.org/10.1128/JB.05982-11.
72. Val M-E, Skovgaard O, Ducos-Galand M, Bland MJ, Mazel D. 2012. Genome engineering in *Vibrio cholerae*: a feasible approach to address biological issues. PLoS Genet 8:e1002472. https://doi.org/10.1371/journal.pgen.1002472.
73. Chiang SL, Rubin EJ. 2002. Construction of a mariner-based transposon for epitope-tagging and genomic targeting. Gene 296:179–185. https://doi.org/10.1016/S0378-1119(02)00856-9.
74. Pierle SA, Rosshandler II, Kerudin AA, Sambono J, Lew-Tabor A, Rolls P, Rangel-Escareño C, Brayton KA. 2014. Genetic diversity of tick-borne rickettsial pathogens; insights gained from distant strains. Pathogens 3:57–72. https://doi.org/10.3390/pathogens3010057.
75. van Opijnen T, Bodi KL, Camilli A. 2009. Tn-seq: high-throughput parallel sequencing for fitness and genetic interaction studies in microorganisms. Nat Methods 6:767–772. https://doi.org/10.1038/nmeth.1377.
76. Baggerly KA, Deng L, Morris JS, Aldaz CM. 2003. Differential expression in SAGE: accounting for normal between-library variation. Bioinformatics 19:1477–1483. https://doi.org/10.1093/bioinformatics/btg173.